PROCEEDINGS, 49th Workshop on Geothermal Reservoir Engineering
Stanford University, Stanford, California, February 12-14, 2024
SGP-TR-227

Techno-Economic Comparison of Different Air-Cooled Condenser Technologies for Geothermal ORC Applications

Lorenzo Galieti[1,3]*, Umberto Merlo[2], Stefano Filippini[2], Dario Alfani[3], Paolo Silva[3]

Paola Bombarda[3], Carlo De Servi[1], Piero Colonna[1]

[1]*Propulsion and Power, Delft University of Technology, Delft, The Netherlands*

[2]*LU-VE s.p.a., Uboldo, Italy*

[3]*Dipartimento di Energia, Politecnico di Milano, Milano, Italy*

*l.galieti@tudelft.nl

Keywords: ORC, air-cooled condenser.

ABSTRACT

Typical binary geothermal power plants employ large fin-fan condensers to ensure the condensation of the organic working fluid. These components are characterized by their substantial size, high construction costs, and the need for extensive on-site carpentry work.

This study focuses on evaluating other viable technologies for geothermal power plants situated in relatively accessible regions. In such areas, the environmental conditions may not demand the level of reliability and robustness associated with fin-fan condensers and it may be preferrable to employ more efficient and easier-to-control solutions. In particular, finned coil condensers, both with and without air pre-humidification, could serve as a valid alternative to condense the working fluid in low-to-medium size binary geothermal power plants, with benefits both in terms of component cost, performance, as well as ease of construction.

To this scope, detailed numerical models that perform the preliminary design of fin-fan condensers and finned coil condensers have been developed with the help of industrial partners and subsequently integrated in an in-house code that simulates ORC power plants. This enabled the optimization of the ORC power plant performance while taking into account various condenser design options and, consequently, a comparison of the two technologies on a cost vs performance basis.

1. INTRODUCTION

Nowadays, binary geothermal power plants based on Organic Rankine Cycles (ORC) are a well-established technology to efficiently convert the brine thermal energy into useful electric power. Their use is usually restricted to water-dominated, low-temperature geothermal sources (Di Pippo, 2005). Because of ecological reasons, ORC power plants typically employ dry air-cooled condensers (Wieland et al., 2023) to cool down and condensate the organic working fluid downstream of the turbine. In geothermal applications, most of the condensers are of the fin-fan type, see for example (Ormat, 2021). These components can be very expensive because of the extensive on-site carpentry work required and, according to different studies, can constitute between 30% (Astolfi et al., 2014) and 80% (Walraven, 2014) of the total installation cost of the ORC surface plant (i.e., geothermal wells and piping excluded). This large discrepancy in the results likely stems from the very different assumptions for the geothermal wells exploration and drilling costs (12M€ and 27M€). Nevertheless, such high share in the plant CAPEX is dictated by the fact that the condenser plays a key role in determining the power plant efficiency, because of the necessity of reducing the cycle minimum temperature as well as the auxiliary fan power consumption, which for air-cooled and low-temperature applications significantly affect the net electricity production of the plant.

Through collaboration with an industrial partner (LU-VE S.p.A, 1986), this work investigates alternative solutions to the conventional fin-fan condenser, which are aimed at medium-sized power plants located in sites where the remarkable robustness of such technology is not required. In particular, the focus is on finned coil condensers that are already in use in other sectors, such as refrigeration. Whilst attaining the condensation of the working fluid by exploiting the same principle (heat exchange through finned tube bundles), this type of condenser presents very substantial differences, most importantly the fact that it is modular, possibly allowing for a significant reduction in the associated manufacturing cost, and thus in the plant investment cost. To assess the benefits of this technology over the most traditional fin-fan one, detailed fin-fan and finned coil condenser models were developed and integrated with an in-house Python tool for the simulation of ORC systems (Galieti et al., 2023)

2. METHODOLOGY

2.1 Thermodynamic cycle modelling

This work considers an air-cooled recuperated ORC power plant for binary geothermal applications. The geothermal brine temperature is set at 150 ºC and the mass flow is 200 kg/s, eventually leading to power plant capacities of 5-6 MW_{el}. No brine reinjection temperature limit was taken into account. Nevertheless, brine leaving temperatures were found to be on the order of 65-70 ºC, which is in line with the usual values assumed in the literature, see for example (Heberle et al., 2016). The working fluid employed in the power plant is isobutane, modelled with the commercial library REFPROP 10 (Lemmon et al, 2018). Ambient air temperature is set to the relatively high value of 30 ºC, to design the condensers at the most demanding conditions. At lower temperatures, operation is guaranteed either by working fluid subcooling or, if inverters are available, by fan speed regulation, each one with their own benefits.

The thermodynamic cycle calculation procedure follows that adopted in (Krempus et al., 2024) and the relevant parameters are reported in Table 1. In particular:

1. Turbomachinery isentropic efficiencies are fixed.
2. Pinch-point temperature differences are fixed in each heat exchanger, except for the condenser.
3. Pressure drops are fixed in each heat exchanger, except for the condenser.

The pressure drops in the air-cooled condenser are calculated with appropriate correlations by the condenser sizing models, which will be presented in the following sub-sections. Given that those models require as input the working fluid thermodynamic conditions at inlet and outlet, which in turn depend on the component pressure drops, and that the actual pressure drops are outputs of the sizing computation, an iterative procedure is required.

The net ORC power output (see equation 1) is chosen as the objective function of the optimization problem. Electrical conversion efficiency has been neglected and the downhole pump consumption has not been included as the analysis is performed considering fixed conditions of the available geothermal fluid.

$$\dot{W}_{net} = \dot{W}_{turb} - \dot{W}_{pump} - \dot{W}_{fan} \tag{1}$$

This methodology is reasonable for geothermal applications because the exploration and drilling of the geothermal wells represent a large share of the project total investment and, for this reason, the ORC power plant is usually designed to attain high conversion efficiency (Astolfi et al., 2014). Optimal cycle parameters are found using the genetic algorithm provided by the optimization suite Pymoo (Blank & Deb, 2020).

Table 1: Thermodynamic cycle assumptions and specifications.

Parameter	Value	Parameter	Value	Parameter	Value
T_{Brine}	150 °C	$\Delta T_{\mathrm{pp}_{PHE}}$	10 °C	η_{pump}	80%
P_{Brine}	25 bar	$\Delta P_{\mathrm{Reg_H}}$	0.025 bar	η_{turbine}	90%
$\Delta P_{\mathrm{PHE_H}}$	0.05 bar	$\Delta P_{\mathrm{Reg_C}}$	$0.025 P_{\mathrm{max}}$	T_{amb}	30 °C
$\Delta P_{\mathrm{PHE_C}}$	$0.025 P_{\mathrm{max}}$	$\Delta T_{\mathrm{pp_{Reg}}}$	10 °C		

2.2 Fin-fan condenser modelling

The outline of a typical fin-fan condenser for geothermal applications is shown in Fig 1. The cooling air flows across a series of finned tube rows, typically made of cast iron, while the condensing fluid flows inside the tubes, following a serpentine path that depends on the tube arrangement. For this study only the tube arrangement reported in Fig 2 was considered, where the first pass has four rows and the second one a single row. This solution limits the pressure drop during the initial de-superheating of the working fluid by splitting the low-density flow between multiple rows, while maintaining a sustained flow velocity (and thus heat transfer coefficient) during condensation, where the working fluid density is progressively increasing.

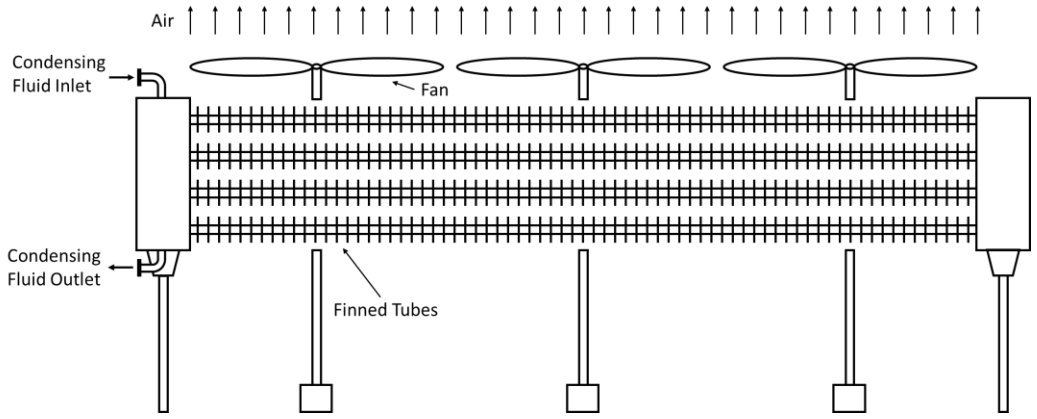

Figure 1: Example of a fin-fan condenser outline

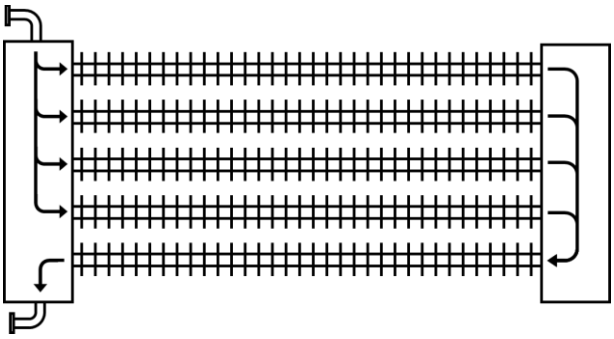

Figure 2: Fin-fan condenser internal flow arrangement considered in this study.

The model handles both superheated and saturated working fluid states. It takes as input the working fluid mass flow rate, inlet and outlet enthalpies, as well as the cooling air temperature and frontal velocity. The latter is the design value of the air velocity at the entrance of the finned tube bank.

The outputs are the heat exchange area, the air-side pressure drop and the frontal area, which is the horizontal area of the heat exchanger through which the air is flowing. The fan power consumption is calculated by assuming a typical value for the overall efficiency of the fans, equal to 60%. A summary of the model inputs, main assumptions, and outputs is provided in Table 2.

The model initially discretizes the heat exchanger into multiple control volumes and for each one solves the heat transfer problem defined by equation 2.

$$\dot{Q} = FUA_{exch}\,\Delta T_{LM} \quad (2)$$

Where $\dot{Q}$ is the heat exchange rate, U is the global heat transfer coefficient, A_{exch} the heat exchange area and ΔT_{LM} the mean logarithmic temperature difference. The global heat transfer coefficient entails three different contributions that take into account convective heat transfer of both fluids as well as heat conduction across the tube wall. The mean logarithmic temperature difference is corrected with a coefficient F to account for the actual heat exchanger configuration, which is not in a purely counterflow arrangement. A summary of the main correlations of the model can be found in Table 3.

Table 2: Inputs, main assumptions and outputs of the fin-fan condenser model.

Input		Input with fixed value		Output	
$P_{out,H}/h_{out,H}$	$\dot{m}_H$	$V_{in,C}$	$2-3\ m/s$	A_{exch}	$\Delta P_{H,update}$
$h_{in,H}$	$\Delta P_{H,guess}$	η_{fan}	60%	A_{frontal}	$\Delta P_{C,update}$
$P_{in,C}/h_{in,C}$	$\Delta P_{C,guess}$			$\dot{W}_{Fan}$	$\dot{m}_C$

The characteristic dimensions of the circular fin tube, see Figure 3, are summarized in Table 4. They were selected based on the manufacturer internal know-how , as well as sources such as (Serth, 2014).

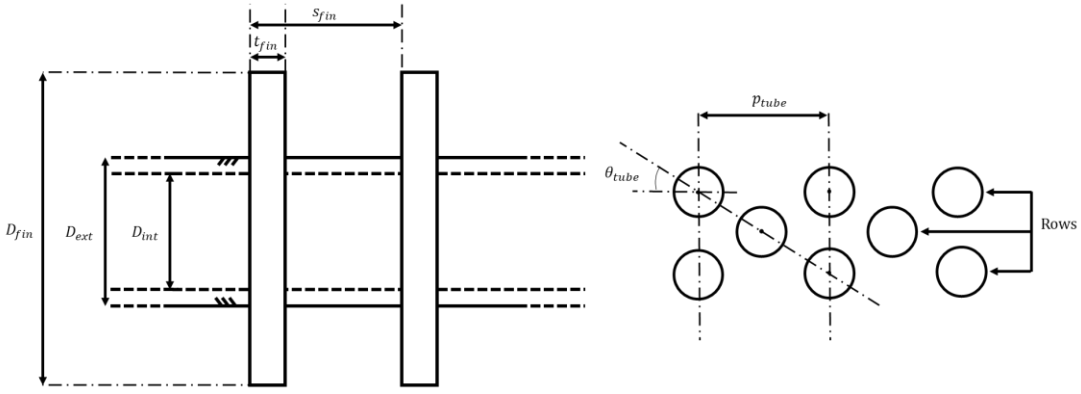

Figure 3: circular fin tube characteristic dimensions

Table 3: Summary of the correlations employed by the model.

Variable	Source	Variable	Source
U_C	Schmidt (VDI-GVC, 2010)	$U_{H,cond}$	Deng (Deng et al., 2019)
$\Delta T_{LM,correction}$	Spang and Roetzel (VDI-GVC, 2010)	$U_{H,desup}$	Gnielinski (VDI-GVC, 2010)
ΔP_{air}	Ganguli (Serth, 2014)	$\Delta P_{H,cond}$	Chilsom (VDI-GVC, 2010)
		$\Delta P_{H,desup}$	Colebrook and White (VDI-GVC, 2010)

Table 4: Circular fin tube characteristic dimensions.

Parameter	Value	Parameter	Value	Parameter	Value
D_{ext}	$25\ mm$	S_{fin}	$2.5 - 2.25^{**}\ mm$	L_{tube}	$12 - 20\ m$
D_{int}	$21\ mm$	t_{fin}	$0.4\ mm$	θ_{tube}	30°
D_{fin}	$56\ mm$	p_{tube}	$60 - 67\ mm$		

** equivalent to 10 and 11 fin per inch respectively.

The associated system of equations is solved with standard numerical methods, many of which are provided by the Python library SciPy (Virtanen et al., 2020). The model was extensively validated in previous works (Galieti et al., 2023) by sizing the condenser for several combinations of working fluids and operating conditions, and then comparing the estimated performance with the predictions of the commercial software Aspen Plus. Table 5 summarizes the main process parameters of an exemplary validation case: the pressure drop is usually the one that attains the largest deviations (in this case 4-5%), especially when selecting medium to high air frontal velocities.

Table 5: Validation of the fin-fan condenser model against Aspen Plus

Parameter	Model	Aspen Plus
$U_C\ (W/m^2K)$	744	730
$\Delta P_C\ (Pa)$	91	95
$\dot{Q}\ (MW)$	32.0	31.8

2.3 Finned coil condenser modelling

The schematic of a typical finned coil is shown in Fig. 4. In contrast with the circular fin tube employed in the fin-fan condenser, the fins are constituted of continuous metal sheets with the tubes inserted perpendicularly. The surface of the fin sheets is corrugated and its shape is optimized for aero-thermal performance. As in the case of the fin-fan condenser, the air flows perpendicularly to the tubes while the condensing fluid follows a serpentine path inside the tubes. In this work, only arrangements with 1 pass (see Figure 4) were considered.

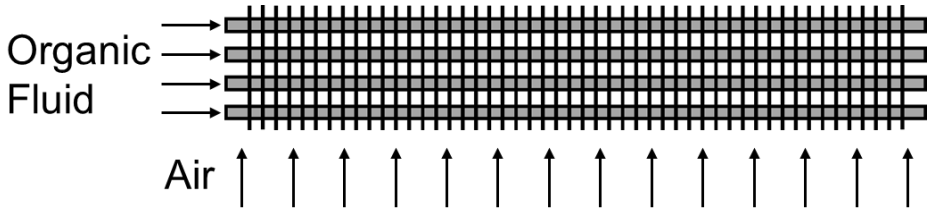

Figure 4: Typical finned coil structure with 3 rows and 1 pass

The tubes are made of copper with a diameter of 10 mm, quite lower than the ones of the fin-fan condenser. The internal surface has a helically grooved structure, that increases the available surface and enhances the flow turbulence to favour the heat exchange process, at the price of a slight increase in the working fluid pressure drop.

In the finned coil condensers considered in this study, two identical coils are installed in a V-shaped arrangement, see Fig 5. Because of simple trigonometric considerations, this arrangement allows for more compact heat exchangers while still containing the air velocity through the fins. Fans are placed at the top of the structure to induce the desired air flow.

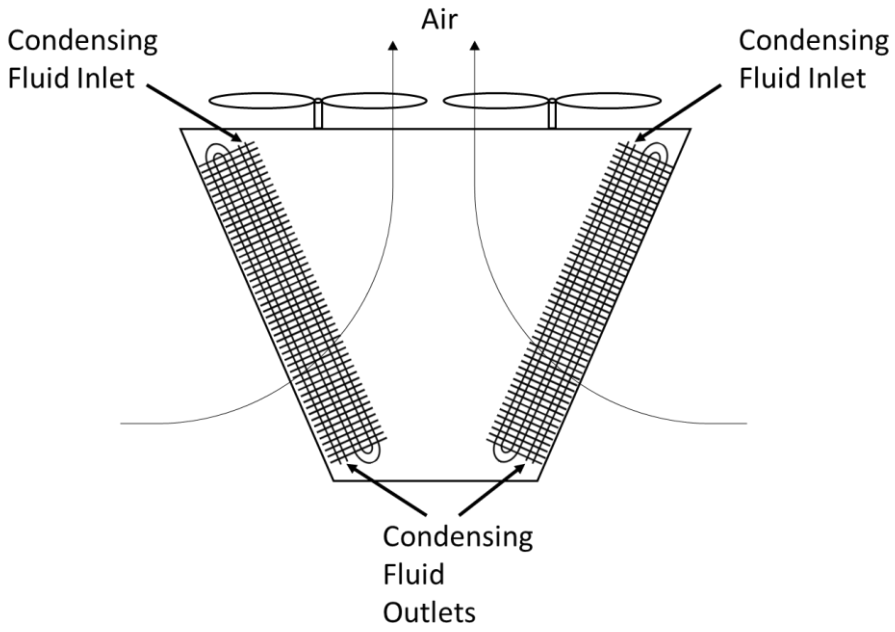

Figure 5: Finned coils arranged in V-Shape.

Multiple V coils can then be placed in parallel together with their respective fans as it can be seen in Fig 6. In practice, the number of coils that can be stacked is limited by the maximum length that allows the machine to be transported on the road, thereby avoiding the need of in-situ carpentry work.

Figure 6: Finned coil condenser with 9 coil couples (and 18 fans) in parallel

In these machines, it is also possible to humidify the cooling air: this may be convenient when high ambient temperatures are expected, as it allows to use a lower number of machines. It can be achieved in two different ways:

1. By pre-humidification at the inlet of the condenser. This is attained by placing porous cellulose sheets (termed pads) in front of the finned coils and soaking them with water. The air flows through the sheets, before entering the condenser and entrailing some of the water, see Fig 7, thereby causing a reduction in air temperature.
2. By directly spraying water over the coils. The evaporation of the water when in contact with the hot metal cools down the tube itself and increases the heat exchanged with the working fluid.

While water spraying on the coil requires the use of demineralized water to avoid tubes and fins corrosion, pre-humidification can be attained with draft water and, for this reason, it was the only option considered in this study. In practice, the hardness of the water sets how often the cellulose sheets need to be replaced.

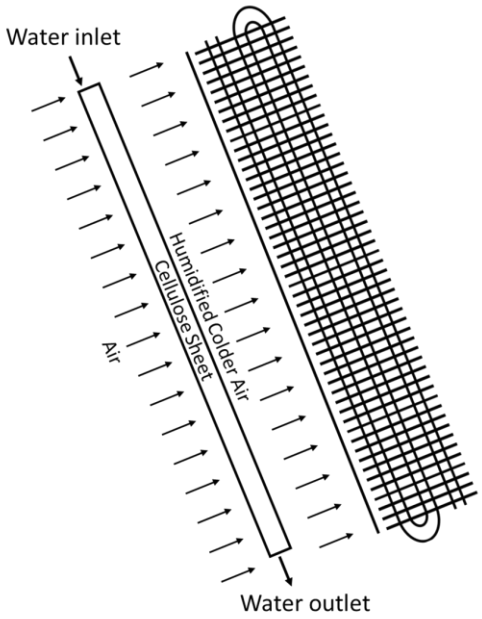

Figure 7: Air pre-humidification by means of soaked cellulose sheets.

Similarly to the fin-fan condenser, the model requires as inputs the working fluid mass flow rate, inlet and outlet enthalpies, as well as the design air temperature. However, in this case, the fan rotational speed defines the cooling air mass flow rate in place of the air frontal velocity of the fin-fan condenser model. The output of the computation is the required number of condensers, the fan power consumption and, should pre-humidification be present, the water consumption. A summary of the model inputs and outputs is provided in Table 6.

Table 6: Inputs and outputs of the finned coil condenser model.

Input		Design Variable	Value	Output	
$P_{out,H}/h_{out,H}$	$\dot{m}_H$	Fan Speed	$70-80-90-100\%$	N_{machines}	$\dot{m}_C$
$h_{in,H}$	$\Delta P_{H,guess}$	Rows	4	$\dot{W}_{Fan}$	$\Delta P_{H,update}$
$P_{in,C}/h_{in,C}$	$\Delta P_{C,guess}$	Ambient relative humidity	40%	Water consumption	$\Delta P_{C,update}$

For what concerns the correlations employed by the model, tube side heat transfer coefficient and pressure drop are calculated using the same ones employed in the fin-fan cooler model. An additional correction for the heat transfer coefficient that considers the effect of the internal helical grooves is included (see (Cavallini et al., 2009)). Pressure drop is instead corrected with a coefficient based on LU-VE company experimental observations. Air side heat transfer coefficient and pressure drop as well as pads performance are determined using industrial partner proprietary experimental fittings.

The model was validated by comparing its predictions against that of LU-VE proprietary software, see Table 7. Note that this preliminary analysis allows for non-integer values of the number of condensers. However, given that such a number is high, errors when estimating the associated costs are not substantial.

Table 7: Validation of the finned coil condenser model against LU-VE proprietary software

Rows/Passes	N. Condensers model	N. Condensers proprietary software
2	36.1	34.6
4	27.5	26.4
4 with Pads	19.5	18.6

3. RESULTS

Figure 8 shows on the Ts (Temperature-specific entropy) diagram the typical thermodynamic cycle of the power plant. The isobutane (black line) exits almost as saturated vapor from the primary heat exchanger, expands in the turbine, passes through the regenerator (see the dashed lines), and then enters the condenser with a substantial degree of superheating. The red and blue lines represent the geothermal fluid and the cooling air, respectively.

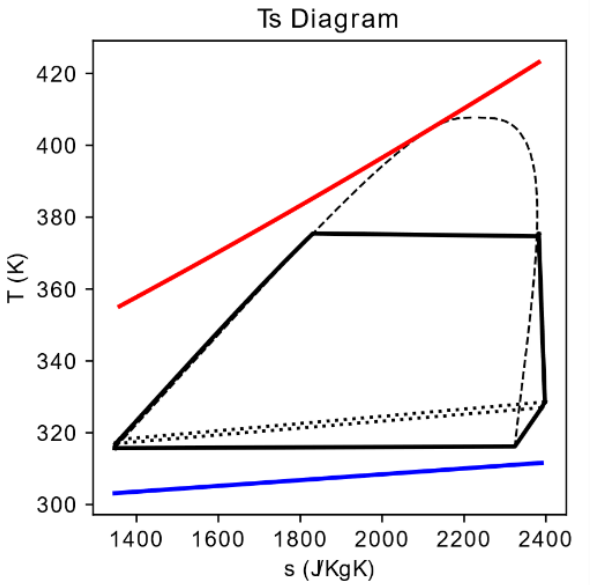

Figure 8: Ts diagram of the typical thermodynamic cycle of the power plant employing isobutane as working fluid.

The optimal condensation pressure is that guaranteeing the best trade-off between the turbine power output and the fan power consumption. The latter is affected by the air side pressure drop, which in turn depends on the air frontal velocity (for the fin-fan condenser) or the fan rotational speed (for the finned-coil condenser). A decrease in one of these two quantities leads to a reduction of the pressure drop and, thus, a reduction of the fan power. Because of the reduction of the fan power, the optimal condensation pressure found by the genetical algorithm will also decrease, allowing for an increased turbine power. At the same time, the condenser air side heat transfer coefficient value will become lower because of the lower air velocity inside the fin banks. Therefore, a larger fin-fan condenser or, equivalently, a greater number of finned-coil condensers will be required. A similar effect can be observed by changing the fin-fan condenser tube pitch or fin spacing, as they ultimately affect the aero-thermal performance of the tube bank. For this reason, all these parameters were considered in a sensitivity study, whose independent variables are reported in Table 8.

Table 8: Condenser design variables considered in a sensitivity study.

	Fin-fan condenser	**Finned coil condenser**
$\boldsymbol{V_{in,C}}$	$2-3\ m/s$	X
$\boldsymbol{S_{fin}}$	$2.5-2.25^{**}\ mm$	X
$\boldsymbol{p_{tube}}$	$60-67\ mm$	X
Fan speed	X	$70-80-90-100\%$

** equivalent to 10 and 11 fin per inch respectively.

3.1 Comparison between fin-fan condenser and finned coil condenser

Figure 9 reports the optimal turbine and fan power as a function of the selected fan rotational speed of the finned coil condensers. As expected, a reduction of the rotational speed has a positive effect on both of them. However, also the number of required condensers increases, see Fig 10, leading to a larger initial investment cost. As such number is already substantial for power plant capacities of 5-7 MW, this indicates that the finned-coil technology could be suitable only for low to medium sized plants.

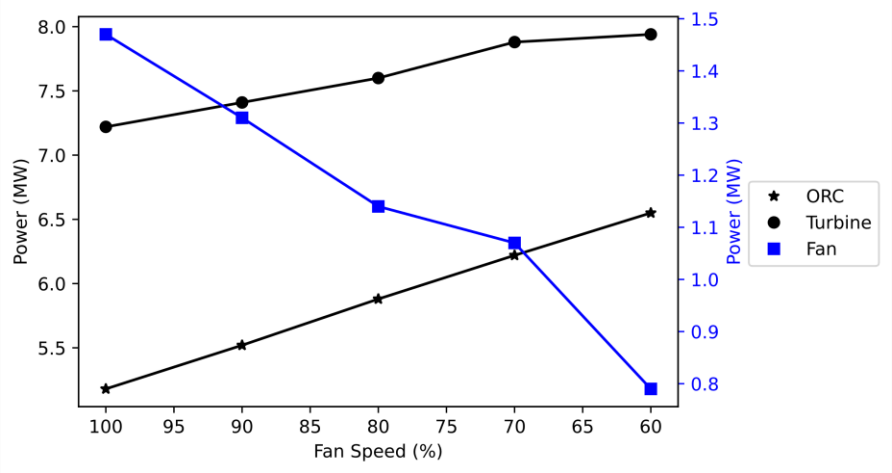

Figure 9: Turbine, fan and net ORC power as function of the selected finned coil condenser fan rotational speed.

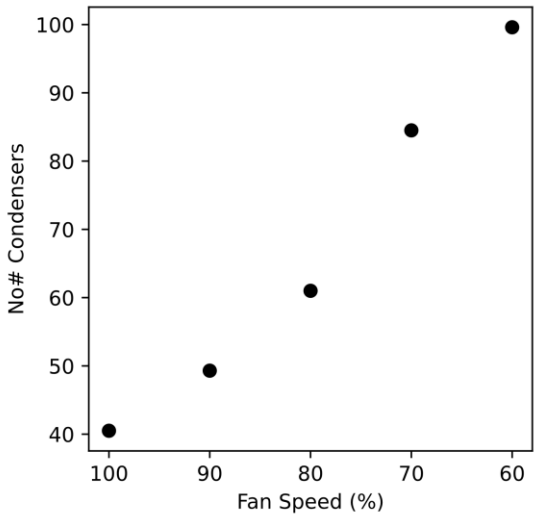

Figure 10: Number of required condensers as a function of the selected finned coil condenser fan rotational speed.

Similar considerations can also be made for the classical fin-fan condenser, as it can be seen in Table 9: a decrease in air frontal velocity or an increase in tube pitch and fin spacing lead to a lower fan consumption and to a higher turbine power, at the expense of an increased number of tubes, leading to more demanding installation costs for the component.

Table 9: Effect of the fin-fan condenser design parameters.

$V_{in,C}\ (m/s)$	$S_{fin}(mm)$	$p_{tube}(mm)$	Net Power (MW)	Fan Power (MW)	Turb. Power (MW)	Number of Tubes
3	2.25	60	4.9	1.36	6.8	11980
2	2.25	60	6.0	1.08	7.7	28778
3	2.5	67	5.3	1.36	7.3	16241
2	2.5	67	6.3	0.98	7.9	34722

To properly compare the two technologies, it is then necessary to carry out a component cost to power analysis, as that highlighted in Fig 11. Multiple sources as well as internal estimates are used to estimate the cost of the fin-fan condenser. The correlation provided in (Hudson Corporation, 2007), which is a fin-fan condenser manufacturer, directly estimates the sales price and agrees reasonably well with Aspen Plus and internal estimates as well as the correlation reported in (Smith, 2005). On the contrary, the method of (Turton, 2012) calculates the price given the size and materials of the component and then uses some coefficients to account for different additional expenses. The method of (Turton, 2012) appears to largely underestimate the cost of the component.

For what concerns finned coil condensers instead, retail prices are reported without considering any economy of scale effect: for these high number of machines, it is expected that the actual selling price will be lower, potentially leading to substantial installation savings with respect to a fin-fan condenser, especially if the sale price reported by (Hudson Corporation, 2007) is taken as the more reliable source. This result is likely reasonable, as the finned coil condenser technology does not require extensive in-situ installation activities because of its modularity.

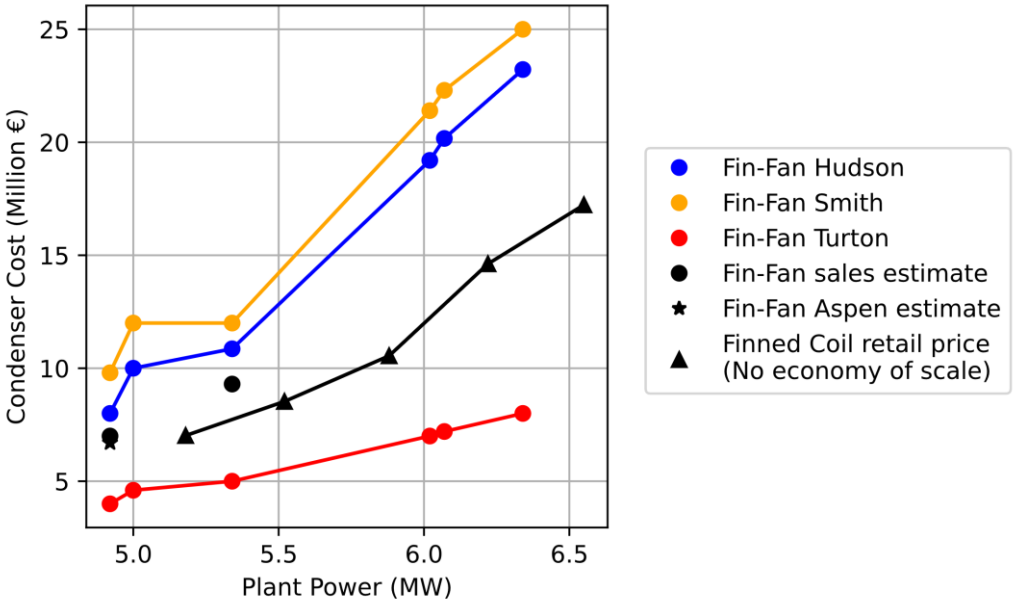

Figure 11: Estimated condenser installation cost (≈2021) as a function of the power plant power output.

Figure 12 reports the internal tube volume for the two technologies, which can provide a rough estimate of the amount of isobutane working fluid residing in the condenser at any given time. Working fluid cost can be relevant in geothermal power plants, as also reported in (Macchi, 2016). The total internal volume of the finned-coil condensers is about half, indicating substantial reductions in working fluid charge, especially because the air-cooled condenser is by far the largest component of the power plant and it also contains condensing fluid, thus partially if not totally liquid, and with high density.

Figure 13 shows the footprint of the condensers: in the case of the fin-fan one, this is just the heat exchanger frontal area. In the case of the finned coil condenser instead, it is assumed that the machines are on the ground arranged in spaced lines, separated by a distance equal to the width of one machine (see Fig 14). This is necessary to ensure that the condensers have enough space to breathe in the required air mass flow rate. it is possible to reduce the distance between the condensers by elevating them and placing them over a supporting structure. However, the assessment of such a solution would require the investigation of the tradeoff between footprint (or terrain) cost and component cost, which is beyond the scope of this study. If the machines are placed on the ground, that is when they occupy the maximum possible space, the footprint of the fin-fan condensers and those with finned-coils are comparable, as shown in Figure 13.

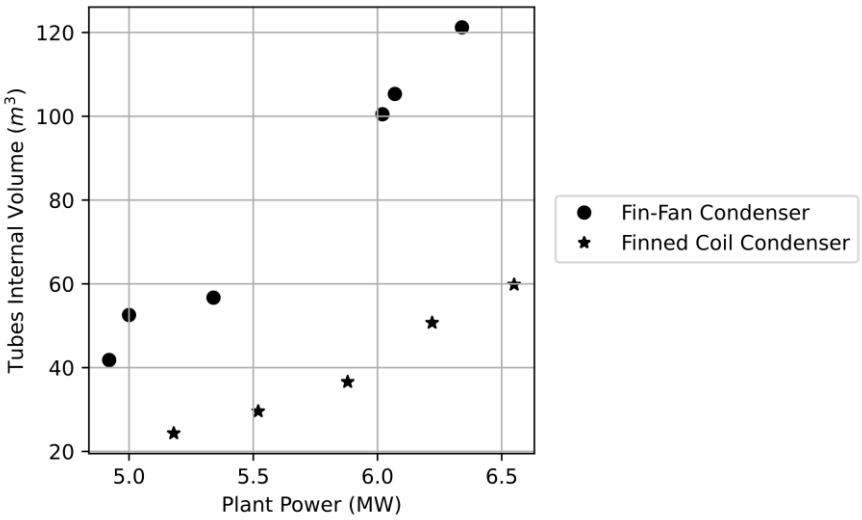

Figure 12: Estimated condenser internal volume as a function of the power plant power output.

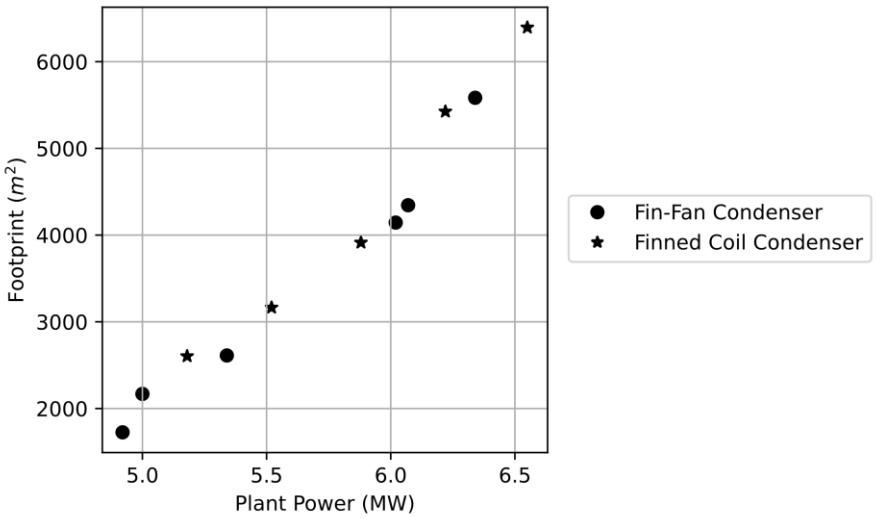

Figure 13: Estimated condenser footprint as a function of the power plant power output.

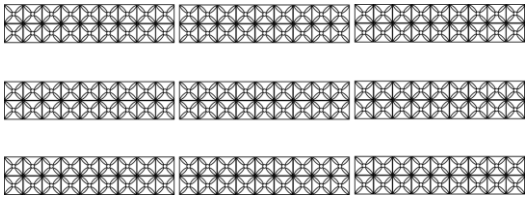

Figure 14: Finned coil condensers arranged on the ground.

3.2 Finned coil condenser air pre-humidification

Figure 15 compares the number of finned-coil condensers that are required to achieve a specific power output when air pre-humidification is adopted. The humidification effectively reduces the inlet air temperature, thus increasing the temperature differences in the machine and promoting the heat exchange. For this reason, a substantial reduction in number of condensers (-20%) can be attained.

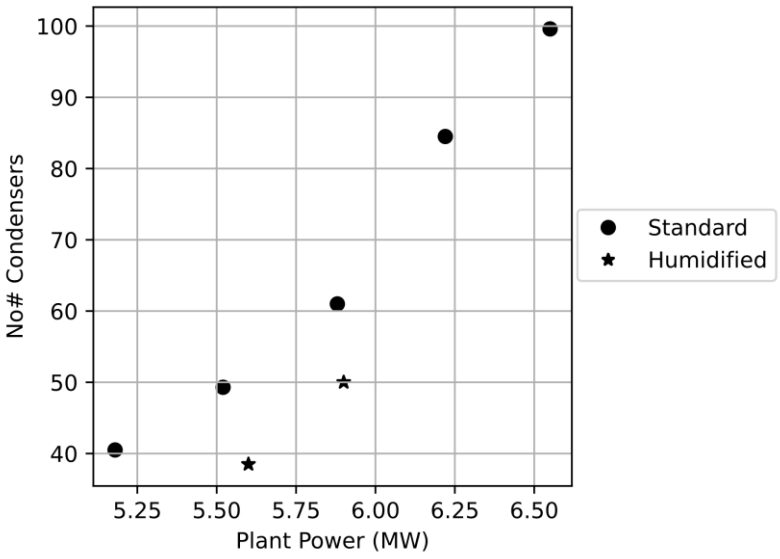

Figure 15: Number of finned coil condensers with and without air pre-humidification for different power plant power outputs

At the same time, this reduction in initial investment cost comes at the expense of water consumption during operation. In practice, the humidification would be carried out only when the ambient temperature is above a predefined value (e.g. 20-25 ºC) while for the remaining

time the condenser would operate normally. This could prove useful, for example, in regions of central Europe, such as Bavaria, where ambient temperature is relatively cold throughout the year, but reaches quite high values during summer (see for example data in (Müller & Floor, 2015). Table 10 reports the water consumption of the finned coil condensers and compares it to that of an equivalent water-cooled power plant, namely adopting a water cooled condenser . In particular the estimate of the water consumption of such a plant, is performed by assuming available cooling water (for example from a river) at 15 ºC and allowing for a theoretical condenser pinch-point temperature difference of 0 ºC, see Fig 16, thus providing a lower bound for the actual water consumption of the plant. It can be noted that even if the water consumption is not negligible, it is significantly less than what is required by direct water cooling solutions.

Table 10: Comparison between the water consumption of the humidified finned coil condensers and a direct water-cooling solution

	Water Consumption (l/h)	Water Consumption (** People equivalent)
Fan Speed 100%	83.000	13.833
Fan Speed 90%	108.000	18.000
Direct Water Cooling	1.800.000	300.000

** Based on an hourly average water consumption of 6 liters per person (European Environment Agency, 2018)

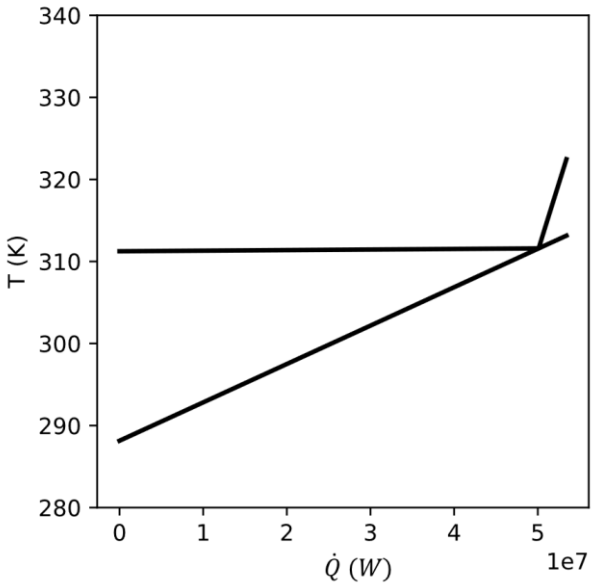

Figure 16: Direct water-cooling ideal condenser TQ (temperature-thermal power) diagram

CONCLUSIONS

Two different types of air-cooled condenser technologies have been modelled with the help of an industrial partner and integrated with an in-house tool that simulates Organic Rankine Cycles. The first technology is the well-established fin-fan air-cooled condenser, which constitutes the mainstream solution currently in use in binary geothermal applications. The second one is instead the finned-coil air-cooled condenser , which is modular and employs more sophisticated geometries and operational strategies. The main findings are as follows:

- Finned coil condensers enable a reduction of the amount of working fluid required to operate the binary power plant as compared to fin-fan condensers, potentially leading to substantial savings in investment costs.
- The footprints of the two condenser technologies are comparable if the finned coil condensers are placed on the ground, thus requiring substantial spacing to breathe in the necessary air mass flow. Elevating them would allow for a reduction in the occupied space, but at the expense of an additional investment to realize the supporting structure.
- The number of fin-fan condensers required for a typical binary geothermal power plant with a capacity of 5-6 MW is high, limiting the application of such technology to low-to-medium size plants because of complexity considerations.
- The plant power output as a function of the price of the finned coil condensers is arguably higher than what can be obtained with a fin-fan condenser, suggesting that it could be beneficial to use them in low-to-medium size power plants.
- Humidification on the cooling air can reduce the required number of finned coil condensers, with possible benefits in terms of complexity and footprint of the power plant. At the same time, the water consumption is not negligible, despite being significantly lower than what would be required in a purely water-cooled solution.

AKNOWLEDGMENTS

This project has received funding from the European Union's Horizon 2020 research and innovation program under the Marie Skłodowska-Curie grant agreement No 956965. This manuscript reflects only the authors' views and opinions, neither the European Union nor the European Commission can be considered responsible for them.

This study was carried out within the NEST - Network 4 Energy Sustainable Transition (D.D. 1243 02/08/2022, PE00000021) and received funding under the National Recovery and Resilience Plan (NRRP), Mission 4 Component 2 Investment 1.3, funded from the European Union - NextGenerationEU. This manuscript reflects only the authors' views and opinions, neither the European Union nor the European Commission can be considered responsible for them.

REFERENCES

Astolfi, M., Romano, M. C., Bombarda, P., & Macchi, E. (2014). Binary ORC (Organic Rankine Cycles) power plants for the exploitation of medium-low temperature geothermal sources - Part B: Techno-economic optimization. *Energy*, *66*, 435–446. https://doi.org/10.1016/j.energy.2013.11.057

Blank, J., & Deb, K. (2020). *Pymoo: Multi-Objective Optimization in Python*. https://doi.org/10.1109/ACCESS.2020.2990567

Cavallini, A., Del Col, D., Mancin, S., & Rossetto, L. (2009). Condensation of pure and near-azeotropic refrigerants in microfin tubes: A new computational procedure. *International Journal of Refrigeration*, *32*(1), 162–174. https://doi.org/10.1016/j.ijrefrig.2008.08.004

Deng, H., Rossato, M., Fernandino, M., & Del Col, D. (2019). A new simplified model for condensation heat transfer of zeotropic mixtures inside horizontal tubes. *Applied Thermal Engineering*, *153*, 779–790. https://doi.org/10.1016/j.applthermaleng.2019.02.128

Di Pippo, R. (2005). *Geothermal Power Plants*. Elsevier. https://doi.org/10.1016/B978-1-85617-474-9.X5029-8

European Environment Agency. (2018). *Water use in Europe, Quantity and quality face big challenges*.

Galieti, L., De Servi, C., Alfani, D., Silva, P., Bombarda, P., & Colonna, P. (2023). On Air-Cooled Condenser for ORC Systems Operating With Zeotropic Mixtures. In *International Seminar on ORC Power Systems*.

Heberle, F., Schifflechner, C., & Brüggemann, D. (2016). Life cycle assessment of Organic Rankine Cycles for geothermal power generation considering low-GWP working fluids. *Geothermics*, *64*, 392–400. https://doi.org/10.1016/j.geothermics.2016.06.010

Hudson Corporation. (2007). *The Basics of AIR-COOLED HEAT EXCHANGERS HUDSON Products Corporation*. www.hudsonproducts.com

Krempus, D., Bahamonde, S., van der Stelt, T. P., Klink, W., Colonna, P., & De Servi, C. M. (2024). On mixtures as working fluids of air-cooled ORC bottoming power plants of gas turbines. *Applied Thermal Engineering*, *236*. https://doi.org/10.1016/j.applthermaleng.2023.121730

LU-VE S.p.A. (1986). *https://www.luvegroup.com/en/*.

Macchi, Ennio. (2016). *Organic Rankine Cycle (ORC) Power Systems*. Elsevier Science.

Müller, G., & Floor, R. (2015). *https://www.wetterzentrale.de/*. https://www.wetterzentrale.de/

Ormat. (2021). *Ormat power plant in the US*. https://www.youtube.com/watch?v=rc-ylzGS1wA&t=245s

Serth, R. (2014). *Process Heat Transfer*. Elsevier. https://doi.org/10.1016/C2011-0-07242-3

Smith, R. (2005). *Chemical Process Design and Integration*.

Turton, Richard. (2012). *Analysis, synthesis, and design of chemical processes*. Prentice Hall.

VDI-GVC. (2010). VDI Heat Atlas. In *VDI Heat Atlas*. Springer Berlin Heidelberg. https://doi.org/10.1007/978-3-540-77877-6

Virtanen, P., Gommers, R., Oliphant, T. E., Haberland, M., Reddy, T., Cournapeau, D., Burovski, E., Peterson, P., Weckesser, W., Bright, J., van der Walt, S. J., Brett, M., Wilson, J., Millman, K. J., Mayorov, N., Nelson, A. R. J., Jones, E., Kern, R., Larson, E., … Vázquez-Baeza, Y. (2020). SciPy 1.0: fundamental algorithms for scientific computing in Python. *Nature Methods*, *17*(3), 261–272. https://doi.org/10.1038/s41592-019-0686-2

Walraven, D. (2014). *Optimization of the Energy Conversion Starting from Low-Temperature Heat Application to Geothermal Binary Cycles*.

Wieland, C., Schifflechner, C., Dawo, F., & Astolfi, M. (2023). The organic Rankine cycle power systems market: Recent developments and future perspectives. *Applied Thermal Engineering*, *224*. https://doi.org/10.1016/j.applthermaleng.2023.119980